4-12-2022

Two *Magnaporthe* appressoria-specific (MAS) proteins, MoMas3 and MoMas5, are required for suppressing host innate immunity and promoting biotrophic growth in rice cells

Ziwen Gong

Na Ning

Zhiqiang Li

Xin Xie

Richard Wilson

See next page for additional authors

Authors

Ziwen Gong, Na Ning, Zhiqiang Li, Xin Xie, Richard Wilson, and Wende Liu

Received: 28 February 2022 | Revised: 12 April 2022 | Accepted: 12 April 2022

DOI: 10.1111/mpp.13226

Molecular Plant Pathology WILEY

ORIGINAL ARTICLE

Two *Magnaporthe* appressoria-specific (MAS) proteins, MoMas3 and MoMas5, are required for suppressing host innate immunity and promoting biotrophic growth in rice cells

Ziwen Gong[1,2] | Na Ning[1,3] | Zhiqiang Li[1] | Xin Xie[3] | Richard A. Wilson[2] | Wende Liu[1]

[1]State Key Laboratory for Biology of Plant Diseases and Insect Pests, Institute of Plant Protection, Chinese Academy of Agricultural Sciences, Beijing, China

[2]Department of Plant Pathology, University of Nebraska-Lincoln, Lincoln, Nebraska, USA

[3]Key Laboratory of Agricultural Microbiology, College of Agriculture, Guizhou University, Guiyang, China

Correspondence
Richard Wilson, Department of Plant Pathology, University of Nebraska-Lincoln, Lincoln, NE, USA.
Email: rwilson10@unl.edu

Wende Liu, State Key Laboratory for Biology of Plant Diseases and Insect Pests, Institute of Plant Protection, Chinese Academy of Agricultural Sciences, Beijing 100193, China.
Email: wendeliu@126.com

Funding information
funding from China Scholarship Council, Grant/Award Number: 201903250119; Pests and Diseases Green Prevention and Control Major Special Project, Grant/Award Number: 110202101045 (LS-05)

Abstract

In the devastating rice blast fungus *Magnaporthe oryzae*, six *Magnaporthe* appressoria-specific (MAS) proteins are encoded by *MoGAS1*, *MoGAS2* and *MoMAS3–MoMAS6*. *MoGAS1* and *MoGAS2* were previously characterized as *M. oryzae* virulence factors; however, the roles of the other four genes are unknown. Here, we found that, although the loss of any *MAS* gene did not affect appressorial formation or vegetative growth, Δ*Momas3* and Δ*Momas5* mutant strains (but not the others) were reduced in virulence on susceptible CO-39 rice seedlings. Focusing on Δ*Momas3* and Δ*Momas5* mutant strains, we found that they could penetrate host leaf surfaces and fill the first infected rice cell but did not spread readily to neighbouring cells, suggesting they were impaired for biotrophic growth. Live-cell imaging of fluorescently labelled MoMas3 and MoMas5 proteins showed that during biotrophy, MoMas3 localized to the apoplastic compartment formed between fungal invasive hyphae and the plant-derived extra-invasive hyphal membrane while MoMas5 localized to the appressoria and the penetration peg. The loss of either *MoMAS3* or *MoMAS5* resulted in the accumulation of reactive oxygen species (ROS) in infected rice cells, resulting in the triggering of plant defences that inhibited mutant growth in planta. Δ*Momas3* and Δ*Momas5* biotrophic growth could be remediated by inhibiting host NADPH oxidases and suppressing ROS accumulation. Thus, MoMas3 and MoMas5 are novel virulence factors involved in suppressing host plant innate immunity to promote biotrophic growth.

KEYWORDS
apoplastic effector, *Magnaporthe* appressoria-specific (MAS) proteins, *Magnaporthe oryzae*, plant immunity, virulence factor

1 | INTRODUCTION

The ascomycete fungus *Magnaporthe oryzae* (synonym *Pyricularia oryzae*) (Wilson, 2021) is a hemibiotrophic plant pathogen that causes blast, the most devastating disease of cultivated rice. Blast disease reduces rice production by approximately 10%–30% per year (which amounts to food for 60 million people) (Wilson & Talbot, 2009). *M. oryzae* not only infects rice but also invades other economically important crops such as wheat and millet (Ou, 1985). In recent years, wheat blast has occurred in Bangladesh and has been threatening

wheat production in South Asia due to the ease by which spores are spread by wind or water droplets (Islam et al., 2016). Thus, studying *M. oryzae* is critical for the management of several important crop diseases.

In nature, plants carry a two-layer immune system that prevents infection by various pathogens or microbes. Pattern-recognition receptors (PRRs) are located on the cell surface of the host to recognize pathogen-associated molecular patterns (PAMPs) derived from pathogens, which activate plant immune responses. This process is the first layer of plant defence, called PAMP-triggered immunity (Jones & Dangl, 2006). For instance, bacterial flagellin peptide flg22 is recognized by the PRR FLS2 in *Arabidopsis*; subsequently, FLS2 interacts with BAK1 to form a signalling complex to trigger plant defence responses (Heese et al., 2007). Another well-known PAMP, chitin (derived from the fungal cell wall), is recognized by CEBiP and CERK1 receptors, which contain an extracellular Lysin motif domain. This induces a series of plant defences, such as callose accumulation and reactive oxygen species (ROS) generation via an oxidative burst (van den Burg et al., 2006; Mentlak et al., 2012). However, to successfully colonize plants, pathogens produce and secrete effectors to subvert PAMP-triggered immunity. Certain effectors are recognized by cognate resistance (R) proteins in plants to induce a strong and robust immune response called effector-triggered immunity, the second layer of plant immunity, which is accompanied by host cell death or the hypersensitive response (Jones & Dangl, 2006). For example, AvirPita in *M. oryzae* is recognized by the R gene *Pita* in rice plants (Orbach et al., 2000).

Depending on where the pathogen effector fulfils its function, effectors can be classified into apoplastic or cytoplasmic. Apoplastic effectors remain outside plant cells and in *M. oryzae* are secreted into the extra-invasive hyphal membrane compartment via the conventional endoplasmic reticulum (ER) to Golgi secretion system. In contrast, in *M. oryzae*, cytoplasmic effectors are secreted via an unconventional pathway into the biotrophic interfacial complex before translocation into host plant cells (Giraldo et al., 2013).

GAS1 and *GAS2* have been identified as virulence factors that are critical for rice infection by *M. oryzae*. Disruption of *MoGAS1* and *MoGAS2* does not inhibit fungal growth, conidiation, or appressorium formation, but these mutants are defective in penetration and the expansion of invasive hyphae in host cells (Xue et al., 2002). The homologs of *GAS1* and *GAS2*, MGG_00703 and MGG_09875, were previously characterized in the *M. oryzae* wild-type strain Ina72 in a large-scale gene deletion study where the disruption of these two genes was reported to have no effect on the pathogenicity of *M. oryzae* in the susceptible rice cultivar Shin No. 2 (Saitoh et al., 2012), although infected leaves were not shown and lesion counting was not performed. Thus, the functions of Gas1 and Gas2 paralogs in *M. oryzae* wild-type strain Guy11 is still unknown. RNAi silencing in *Podosphaera* of effectors with chitinase activity (EWCAs), the homologs of *GAS1* and *GAS2* in powdery mildew fungi, induced the plant immunity response and delayed invasive hyphal development, suggesting conserved roles for *GAS1* and *GAS2* homologs in pathogenicity (Martínez-Cruz et al., 2021). However, in general, little is known about the function of these proteins in pathogenicity.

To shed light on the factors required by *M. oryzae* to colonize host rice cells, in this study we analysed four other paralogs of *GAS1* and *GAS2*, namely *MoMAS3*, *MoMAS4*, *MoMAS5*, and *MoMAS6*, which have unknown functions. The genes were characterized in *M. oryzae* via a combination of methods, including the split-PCR strategy for targeted gene deletion, spray inoculations, leaf sheath assays, protein localization studies, and gene expression analysis. Our data indicate that *MoMAS3–MoMAS6* are expressed in appressoria and in the early infection stage, and encode proteins containing N-terminal signal peptides that share a conserved domain in filamentous fungi. In addition, deletion of *MoMAS3* or *MoMAS5* resulted in a reduction in pathogenicity due to the restriction of invasive hyphae caused by reactive oxygen species (ROS) accumulation in infected rice cells. Together, our results suggest that *MoMAS3* and *MoMAS5* encode novel virulence factors that play a critical role in suppressing plant immunity.

2 | RESULTS

2.1 | Identification of MoMas proteins in *M. oryzae*

We analysed and screened our previous transcriptome data for genes encoding putative secreted proteins during the early infection stage of *M. oryzae* (Chen et al., 2013). We identified six genes specifically expressed in *Magnaporthe* appressoria, including MGG_12337 (*MoGAS1*, encoding a protein of 251 amino acids), MGG_04202 (*MoGAS2*, 290 amino acids), MGG_00703 (*MoMAS3*, 322 amino acids), MGG_09875 (*MoMAS4*, 275 amino acids), MGG_02253 (*MoMAS5*, 280 amino acids), and MGG_00992 (*MoMAS6*, 370 amino acids). All six of these genes encode proteins carrying an N-terminal signal peptide and a conserved DUF3129 domain, as determined using the SMART structure domain prediction website (http://smart.embl-heidelberg.de/smart/set_mode.cgi?GENOMIC=1) and signal peptide prediction website (http://www.detaibio.com/tools/signal-peptide.html) (Figure S1a). Protein sequence alignment showed that Mas proteins are rich in Ala and Gly residues (Figure S2). Because Gas1 and Gas2 proteins are exclusive to filamentous fungi (Xue et al., 2002), we used each of the Mas protein sequences to search against the NCBI database using BLAST (https://blast.ncbi.nlm.nih.gov/Blast.cgi) to construct a phylogenetic tree of Mas proteins, including *M. oryzae* (six paralogous proteins), *Colletotrichum graminicola* (six homologous proteins), *Fusarium graminearum* (four homologous proteins), *Alternaria alternata* (four homologous proteins), and *Neurospora crassa* (two homologous proteins). Based on the bootstrap values, these proteins were classified into three clades (Figure S1b), MoGas1 and MoMas4, MoGas2 and MoMas5, and MoMas3 and MoMas6, reflecting that they are the closest paralogues to each other in *M. oryzae*. Overall, these results suggest that Mas proteins may have conserved functions in filamentous fungi.

2.2 | Deletions of targeted genes and characterization of the resulting mutant strains

To understand the biological function of *MAS* genes in fungus–plant interactions, we knocked out each *MoMAS* gene by homologous recombination, and verified their genotypes via PCR and reverse transcription (RT)-PCR with specific primer sets (Table S2), thus obtaining Δ*Momas3*, Δ*Momas4*, Δ*Momas5*, and Δ*Momas6* mutant strains. We also complemented the Δ*Momas3* and Δ*Momas5* mutant strains with the genomic sequence of the *MoMAS3* and *MoMAS5* genes, containing their native promoters.

To determine whether *MoMAS* genes function in vegetative growth, conidia formation, and/or appressoria formation, we tested vegetative growth on a complete medium (CM) plate, conidia formation on oatmeal medium (OM) plates, and appressorium formation on an artificial hydrophobic surface. Compared to the wild-type strain, none of the single deletion mutants showed changes in vegetative growth, sporulation, or appressoria formation (Figures S3 and S4), indicating that *MoMAS* genes are not required for these physiological processes.

2.3 | *MoMAS3* and *MoMAS5* are required for full virulence in *M. oryzae*

To determine whether *MoMAS* genes are involved in the pathogenicity process, we sprayed equivalent conidial suspensions on 2-week-old CO-39 rice seedlings. The results were observed and photographed at 7 days postinoculation (dpi) in rice leaves. We counted the number of lesions per 5 cm length of leaves, and showed that the number of lesions was reduced by 35% and 40% on leaves infected with Δ*Momas3* and Δ*Momas5* mutant strains, respectively, compared to the Δ*Momas3*/*MoMAS3* and Δ*Momas5*/*MoMAS5* complementation strains, which were restored to full pathogenicity like the wild type (WT) (Figure 1a,b) (Student's *t* test, $p < 0.05$). Our data demonstrated that inoculation with the Δ*Momas3* and Δ*Momas5* mutant strains resulted in a significant reduction in lesions compared with the number of lesions caused by infection with the WT strain Guy11, while for Δ*Momas4* and Δ*Momas6* mutants there was no obvious difference in the number of lesions caused by the WT and the mutant strains (Figure S5a,b). These results indicate that *MoMAS3* and *MoMAS5* (but not *MoMAS4* and *MoMAS6*) play critical roles in pathogenicity.

Because only Δ*Momas3* and Δ*Momas5* mutants showed a reduction in virulence, we focused on analysing these two genes in subsequent experiments. To further investigate why the Δ*Momas3* and Δ*Momas5* mutants showed reduced pathogenicity in host plants, we performed detached rice leaf sheath assays to examine the growth of invasive hyphae at 45 h postinoculation (hpi). Invasive hyphal growth in rice leaf sheaths was evaluated using an invasive hyphatype assay (Li et al., 2020a; Wang et al., 2013). The four types (type 1, no penetration; type 2, with a penetration peg; type 3, invasive hypha grows in one cell; type 4, invasive hypha move into adjacent cell) of invasive hyphae were observed in the leaf sheath. In the WT strain, approximately 55% of the cells showed type 4 growth and approximately 40% cells showed type 2 and type 3 growth by 45 hpi. In contrast, in the Δ*Momas3* and Δ*Momas5* mutants approximately 20%–25% cells showed type 4 growth and 60%–65% showed type 2 and type 3 (Figure 2a,b). These results indicated that the disruption of *MoMAS3* and *MoMAS5* affects invasive hyphal growth but not appressorial penetration.

2.4 | Δ*Momas3*/Δ*Momas5* double mutant has a phenotype similar to those of the Δ*Momas3* and Δ*Momas5* single mutants

To determine whether the Δ*Momas3*/Δ*Momas5* double mutant strain has an additive effect in decreasing virulence, we used bleomycin resistance as a screening marker gene to replace *MoMAS3* in the Δ*Momas5* mutant background, with the same strategy that was used in the single deletion *MAS* gene. After PCR and reverse transcription (RT)-PCR identification, we successfully confirmed Δ*Momas3*/Δ*Momas5* double mutants. Two double mutant strains were tested and found to have normal fungal growth, conidiation, and appressorium formation (Table S1). Compared to the WT strain, the disease lesions of the double mutant strain were reduced by 30% (Figure S6a,b), which was similar to results for Δ*Momas3* and Δ*Momas5* single mutants. This finding suggests that the disruption of both *MoMAS3* and *MoMAS5* does not have any additive effect in reducing the virulence of the Δ*Momas3*/Δ*Momas5* double mutant.

2.5 | *MoMAS3* and *MoMAS5* gene expression peaks in the early biotrophic stage

To characterize the potential function of MoMas3 and MoMas5 proteins, we performed RT-quantitative PCR (RT-qPCR) analysis to examine their transcriptional patterns in spores, mycelia, appressoria, and infection stages. We found that the expression levels of *MoMAS3* and *MoMAS5* were up-regulated at the early infection stage at 18 and 24 hpi, followed by a dramatic decrease at 42 hpi. In addition, our results revealed that *MoMAS3*, but not *MoMAS5*, was expressed in the mycelia. Moreover, an extremely low expression of *MoMAS3* was seen in spores, while for *MoMAS5* it was difficult to detect its expression in the conidial stage (Figure 3). These results further suggest that *MoMAS3* and *MoMAS5* are involved in pathogen infection.

2.6 | Subcellular localization of MoMas3 and MoMas5

To determine the subcellular localization of MoMas3 and MoMas5 proteins, the C-termini of MoMas3 and MoMas5 were tagged with green fluorescent protein (GFP). MoMas3-GFP and MoMas5-GFP

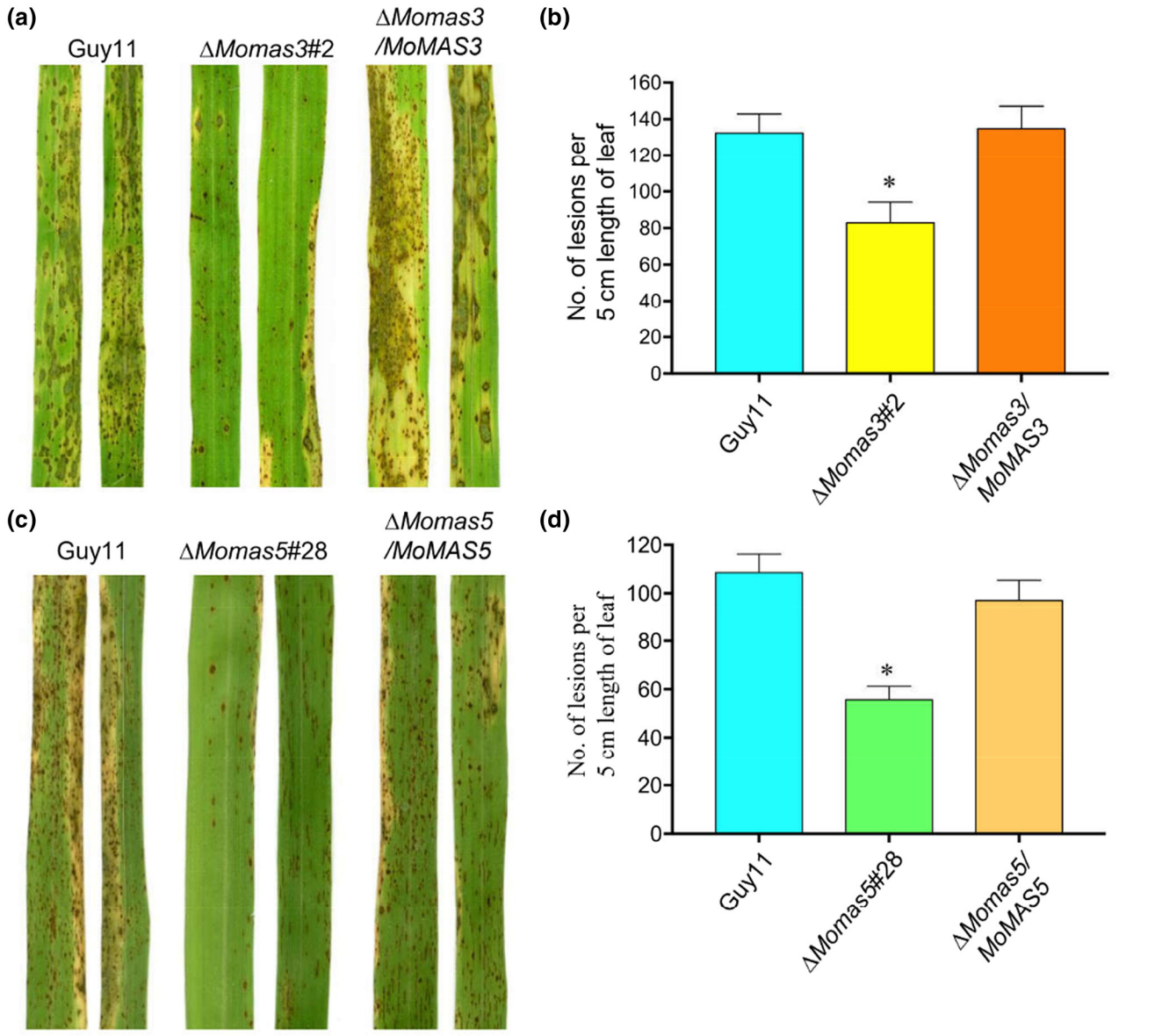

FIGURE 1 *MoMAS3* and *MoMAS5* are required for full virulence of *Magnaporthe oryzae*. (a, c) The pathogenicity of *M. oryzae* is compromised in the Δ*Momas3* and Δ*Momas5* mutants. A conidial suspension (10^5 spores/ml) of *M. oryzae* wild-type Guy11, Δ*Momas3*, Δ*Momas5*, or complementation strains was sprayed onto 3-week-old CO-39 rice seedlings at 25°C for 7 days. Three independent assays were performed. Lesions were photographed and measured at 7 days postinoculation. (b, d) Lesion number on a 5-cm length of rice leaves infected with *M. oryzae* wild-type Guy11, Δ*Momas3*, Δ*Momas5*, and complementation strains. Bar indicates the standard deviation of three replicates, significance of differences was analysed by Student's *t* test ($p < 0.05$), and asterisks indicate significant differences

fusions were transformed into the Δ*Momas3* mutant and Δ*Momas5* mutant strains, respectively. Two transformants of MoMas3-GFP (MoMas3-GFP #15 and #23) and two transformants of MoMas5-GFP (MoMas5-GFP #3 and #12) were identified by PCR. In the infection assay, compared with the mutants, all these GFP fusion strains restored full pathogenicity. There was no obvious difference in conidia, mycelia, vegetative growth, and appressorium formation of MoMas3-GFP and MoMas5-GFP transformants (data not shown). We randomly chose MoMas3-GFP #23 and MoMas5-GFP#3 strains for further analysis.

The spores were harvested and adjusted to 10^5 spores/ml, and conidial suspensions were added to cover slips to check the fluorescence at the indicated time points. In the conidial stage, the stronger green signals of the positive control WT-GFP strain (i.e., WT constitutively producing GFP in the cytoplasm) localized throughout the conidia (Figure S7a). In the MoMas3-GFP strain, the green signals localized to the septum and cell wall, but MoMas5-GFP was not detected under the microscope with the same settings (Figure 4a). We then examined the localization of MoMas3-GFP and MoMas5-GFP in germ tubes and hyphae. The green signal of MoMas3-GFP accumulated in the cytoplasm of germ tubes and hyphae, which was similar to that of the positive control WT-GFP, whereas no signal was detected in the MoMas5-GFP strain (Figures 4b,c and S7c,d).

To check the localization of WT-GFP, MoMas3-GFP, and MoMas5-GFP in the appressorium formation stage at different time points (6,

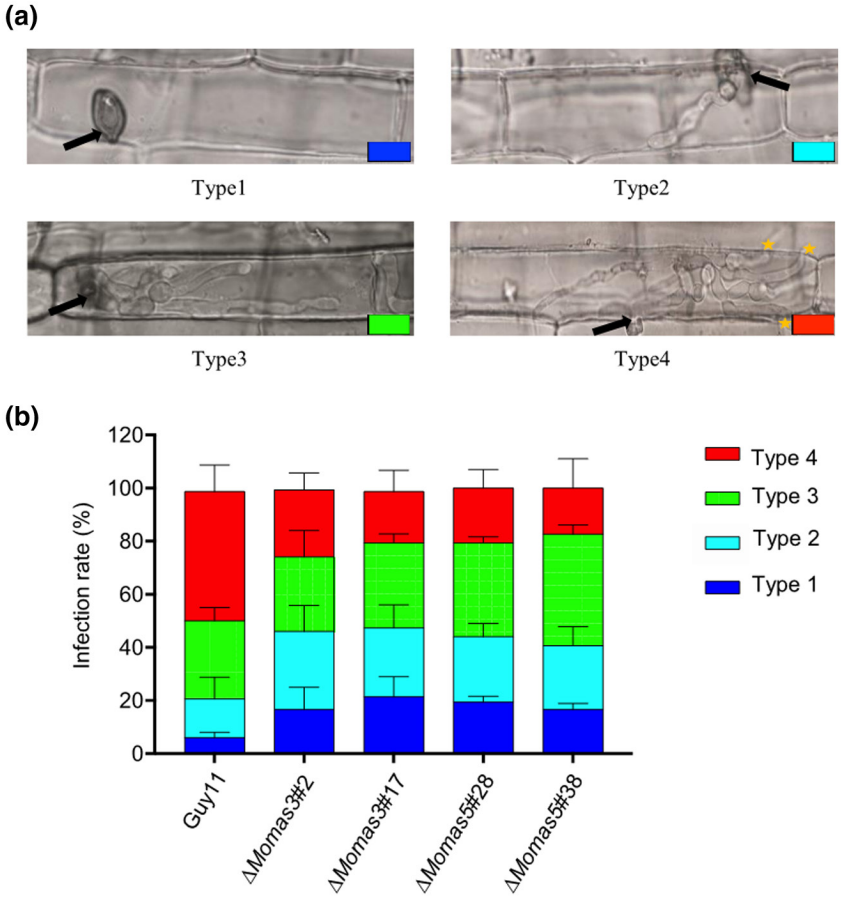

FIGURE 2 Single deletion of *MoMAS3* and *MoMAS5* leads to a restriction of invasive hyphae (IH). (a) Penetration assay was performed in rice leaf sheaths and IH growing in rice cells were observed at 45 h postinoculation. (b) Statistical analysis of each type of IH shape for indicated strains; 50 IH were counted per replicate and the experiment was repeated three times. Type 1, no penetration; type 2, a single or short primary hypha; type 3, IH expanded but restricted in the first infected cell; type 4, IH invading neighbouring cells. Error bars represent standard deviations

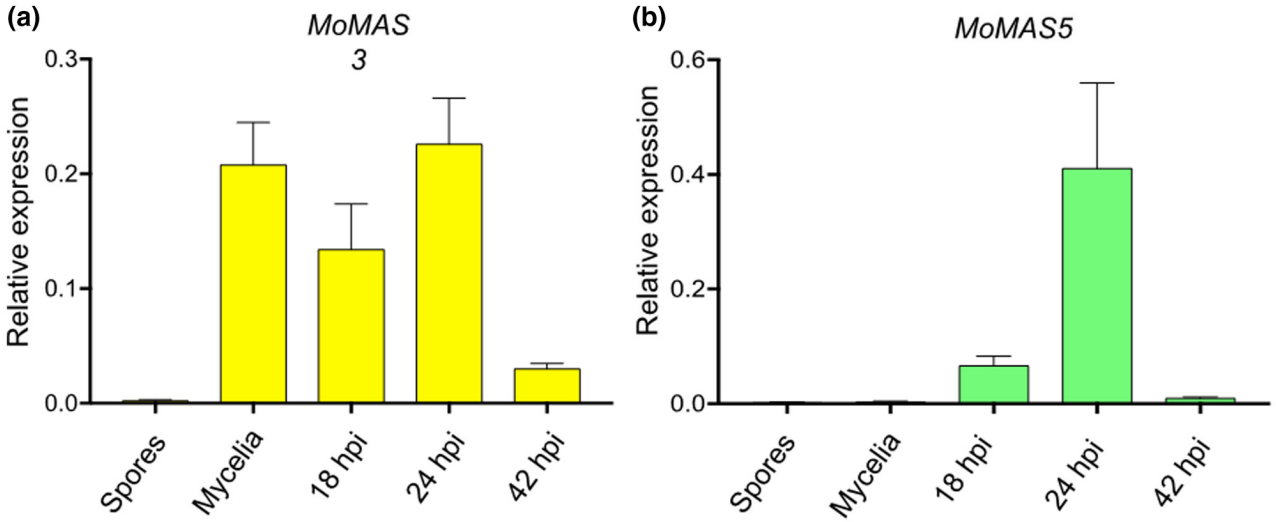

FIGURE 3 *MoMAS3* and *MoMAS5* gene expression peaks in the early infection stage. The expression pattern of *MoMAS3* and *MoMAS5* in spores, mycelia, and at the early infection stage was performed using reverse transcription-quantitative PCR (RT-qPCR). hpi, hours postinoculation. Three independent biological experiments with three replicates each time were performed and similar results were obtained each time. Error bars represent standard deviations

15, and 24 hpi), the conidial suspensions of the indicated strains were added onto a hydrophobic surface at 25°C and observed at the indicated time points. Microscopic observations showed that the green signals of the WT-GFP strain localized to whole conidia and appressoria at 6, 15, and 24 hpi. In contrast, MoMas3-GFP localized to the septum and cell wall at 6 hpi, and a weak signal observed in the cytoplasm of appressoria from 6 to 15 hpi grew slightly stronger by 24 hpi. It was difficult to observe the green fluorescence of MoMas5-GFP at 6 hpi, but from 15 to 24 hpi it localized to a circle inside the appressorium, perhaps surrounding the appressorial pore (Figures 5a,b and S7b).

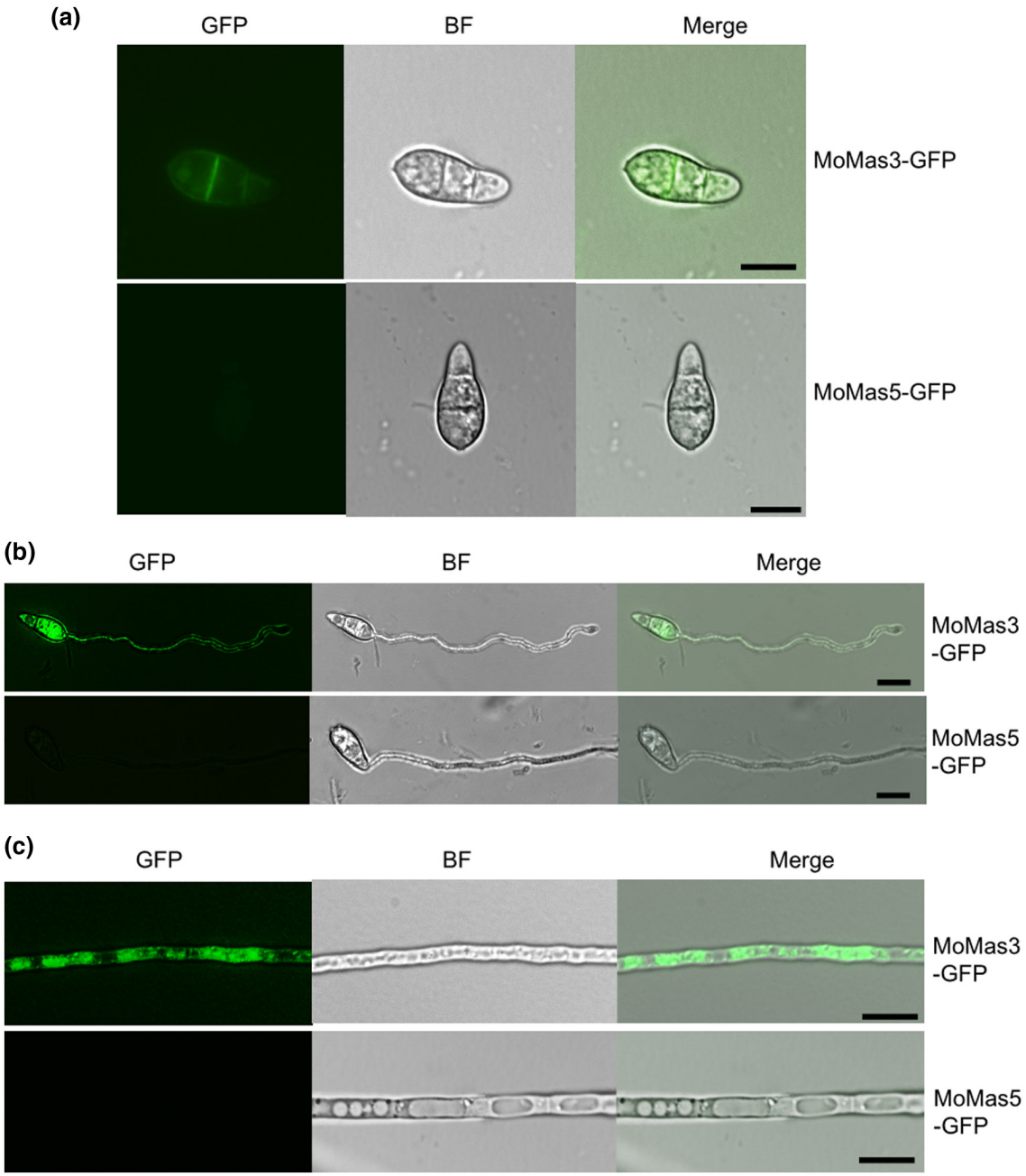

FIGURE 4 MoMas3 (but not MoMas5) is expressed in the cytoplasm and septum in conidia, germ tubes, and mycelia. (a) The localization of MoMas3-GFP and MoMas5-GFP in conidia. (b) The subcellular localization of MoMas3-GFP and MoMas5-GFP in germ tubes was performed on a hydrophilic surface and the results were checked at 6 h postinoculation. (c) The subcellular localization of MoMas3-GFP and MoMas5-GFP in mycelia. Green fluorescence is shown in the left image (GFP). The bright field (BF) microscopy image is shown in the middle. The merge of green fluorescence and bright field is shown on the right (Merge). Bar = 10 μm

2.7 | MoMas3 accumulates in the extra-invasive hyphal membrane compartment, while MoMas5 is weakly localized at the penetration peg

To determine whether MoMas3 and MoMas5 were expressed in the invasive hyphae, conidia were harvested from MoMas3-GFP #23 and MoMas5-GFP #3. Conidial suspensions were injected into the rice leaf sheath, and the localization of MoMas3 and MoMas5 in invasive hyphae at 22, 26, 30, and 36 hpi was observed. In the control strain, GFP localized to the cytoplasm of invasive hyphae from 26 to 42 hpi (Figure S8a). In contrast, the green signals of MoMas3-GFP outlined the invasive hyphae (Figure 6a). This result was similar to that of the classic apoplastic effector Bas4, which is secreted via the conventional ER-Golgi pathway (Giraldo et al., 2013). To examine whether MoMas3 is an apoplastic effector, the leaf sheath infected by the indicated strain at 26 hpi was treated with brefeldin A (BFA). After 3 h of exposure, the green signal was observed inside invasive hyphae (Figure 6b), which indicated that MoMas3 protein cannot be secreted into the apoplast space, while for the control strain the GFP

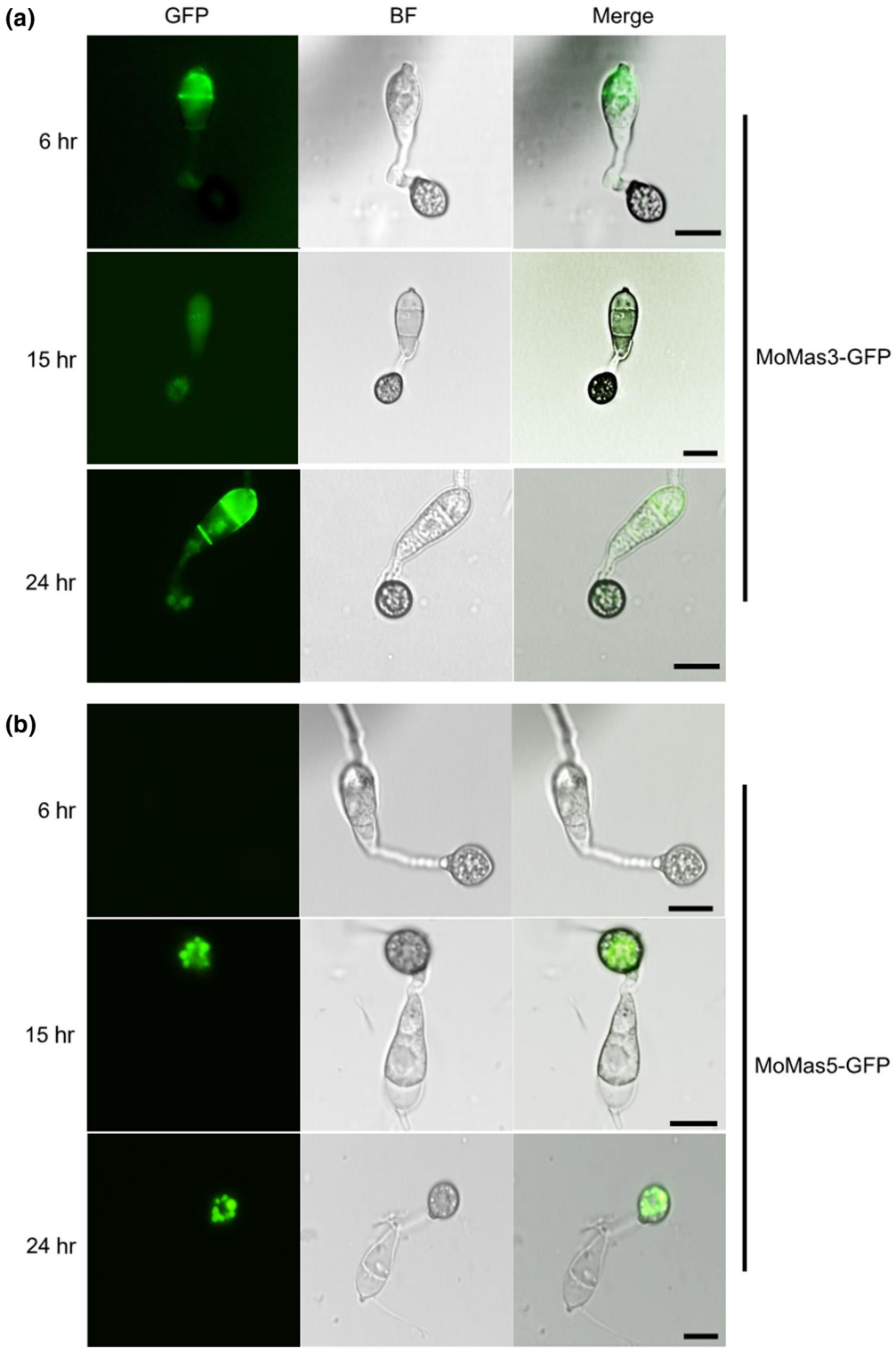

FIGURE 5 Both MoMas3 and MoMas5 localized to the appressorium. (a, b) A time course of localization of MoMas3-GFP and MoMas5-GFP at the appressorial formation stage was performed on an artificial hydrophobic surface, and the results were observed at 6, 15, and 24 h postinoculation (hpi). Bar = 10 μm

signals still localized to the cytoplasm of invasive hyphae after BFA treatment, which is similar to the nontreated controls (Figure S8b). These data suggest that MoMas3 is a secreted apoplastic-localized protein, possibly an effector mediating the *M. oryzae* interaction with rice. In contrast to MoMas3, the strong signals of MoMas5-GFP localized to the cytoplasm of appressoria and extremely weak signals accumulated in the penetration peg during the early infection stage. Interestingly, no signal was observed in the invasive hyphae (Figure 7).

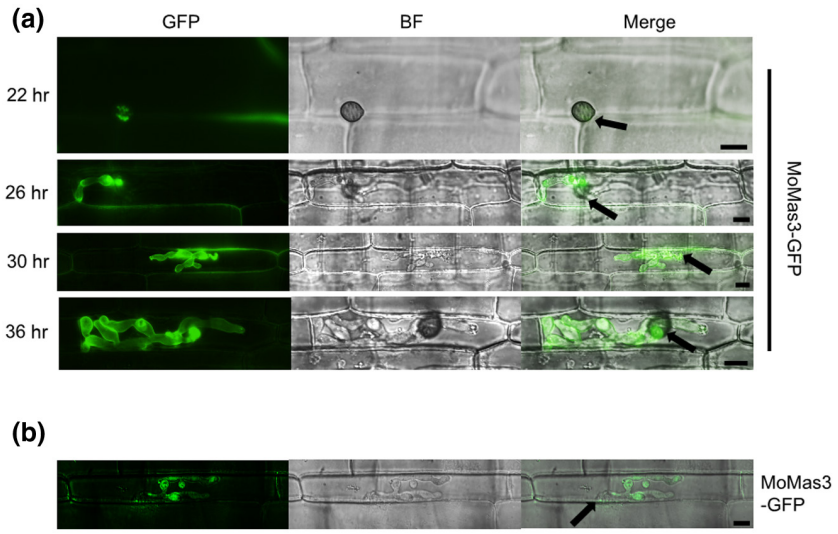

FIGURE 6 MoMas3 outlined the invasive hypha during the biotrophic phase. (a) Live-cell imaging of the leaf sheath infected by indicated strains tagged with green fluorescent protein (GFP) shows that green signals accumulate in the extra-invasive hyphal membrane. (b) A leaf sheath infected with MoMas3-GFP was treated with 10 μg/ml brefeldin A (BFA) at 26 h postinoculation (hpi) and the sample was observed at 29 hpi. Black arrows indicate appressoria. Bar = 10 μm

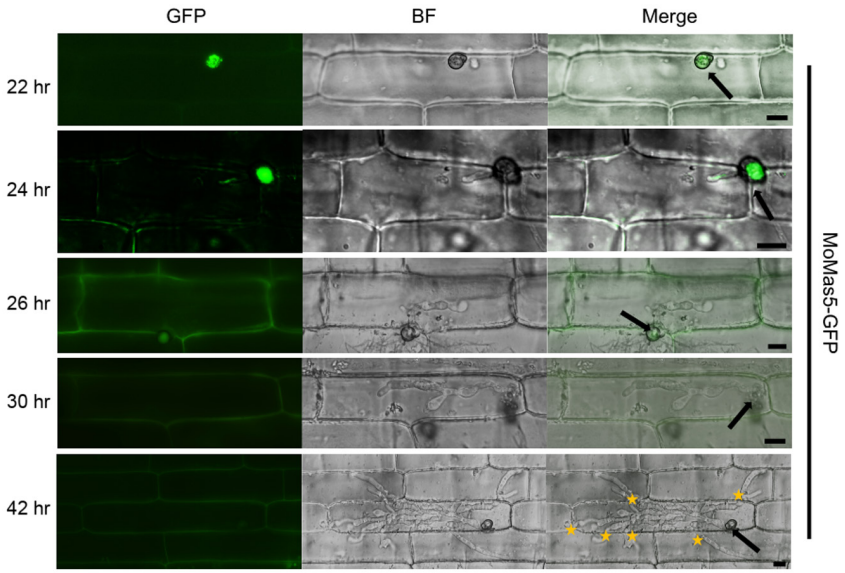

FIGURE 7 MoMas5 localized to the appressorium and penetration peg in rice leaf sheath. Microscopic observation of MoMas5-GFP in rice cells at different time points postinoculation. Black arrows indicate appressoria. Yellow stars represent invasive hyphae invading neighbouring cells. Bar = 10 μm

2.8 | MoMas3 and MoMas5 are involved in suppressing plant immune responses via host ROS scavenging

To determine the mechanisms underlying the reduction of pathogenicity in the Δ*Momas3* and Δ*Momas5* mutants, the detached rice leaf sheath assay was performed to determine with more precision how MoMas3/MoMas5 contribute to infection. We found by 36 hpi that in Δ*Momas3*- and Δ*Momas5*-infected rice cells, most of the mutant invasive hyphae were restricted in the first infected rice cell and black compounds were visible in mutant-infected rice cells, unlike WT-infected rice cells (Figure 8a). Similar black deposits have been observed previously in rice cells infected with mutants unable to neutralize host ROS, which triggers host innate immunity (Fernandez et al., 2014; Li et al., 2020c; Marroquin-Guzman et al., 2017; Rocha & Wilson, 2020). Thus, we hypothesized that ROS could be accumulating at the penetration sites of rice cells infected with Δ*Momas3* or Δ*Momas5*, resulting in the triggering of host defences that inhibited biotrophic growth. To test this, the excised samples from rice leaf sheaths inoculated with Δ*Momas3* and Δ*Momas5*, WT, and complementation strains were stained with 3,3′-diaminobenzidine (DAB) to detect ROS accumulation. We found that 80% of the rice cells infected with Δ*Momas3* and Δ*Momas5* mutants were stained, compared to 20% of those infected with Guy11 strains (Figure 8b,c). These results demonstrate that the Δ*Momas3* and Δ*Momas5* mutants cannot prevent ROS accumulation in infected cells.

It is well known that ROS not only restrict fungal growth but also act as secondary signals to regulate plant defence (Alvarez et al., 1998; Lamb & Dixon, 1997; Zhang et al., 2009). Diphenyleneiodonium (DPI), an inhibitor of NADPH oxidase, is used to inhibit ROS generation in plants (Guo et al., 2019; Marroquin-Guzman et al., 2017; Wang et al., 2017). Thus, we treated infected rice leaf sheaths with DPI. When the leaf sheath was infected with conidia suspension containing 0.4 μM DPI for 36 hpi, the invasive hyphae of the Δ*Momas3* and Δ*Momas5* mutants were restored for growth and spread to adjacent cells, and the black deposits were no longer visible (Figure 8d).

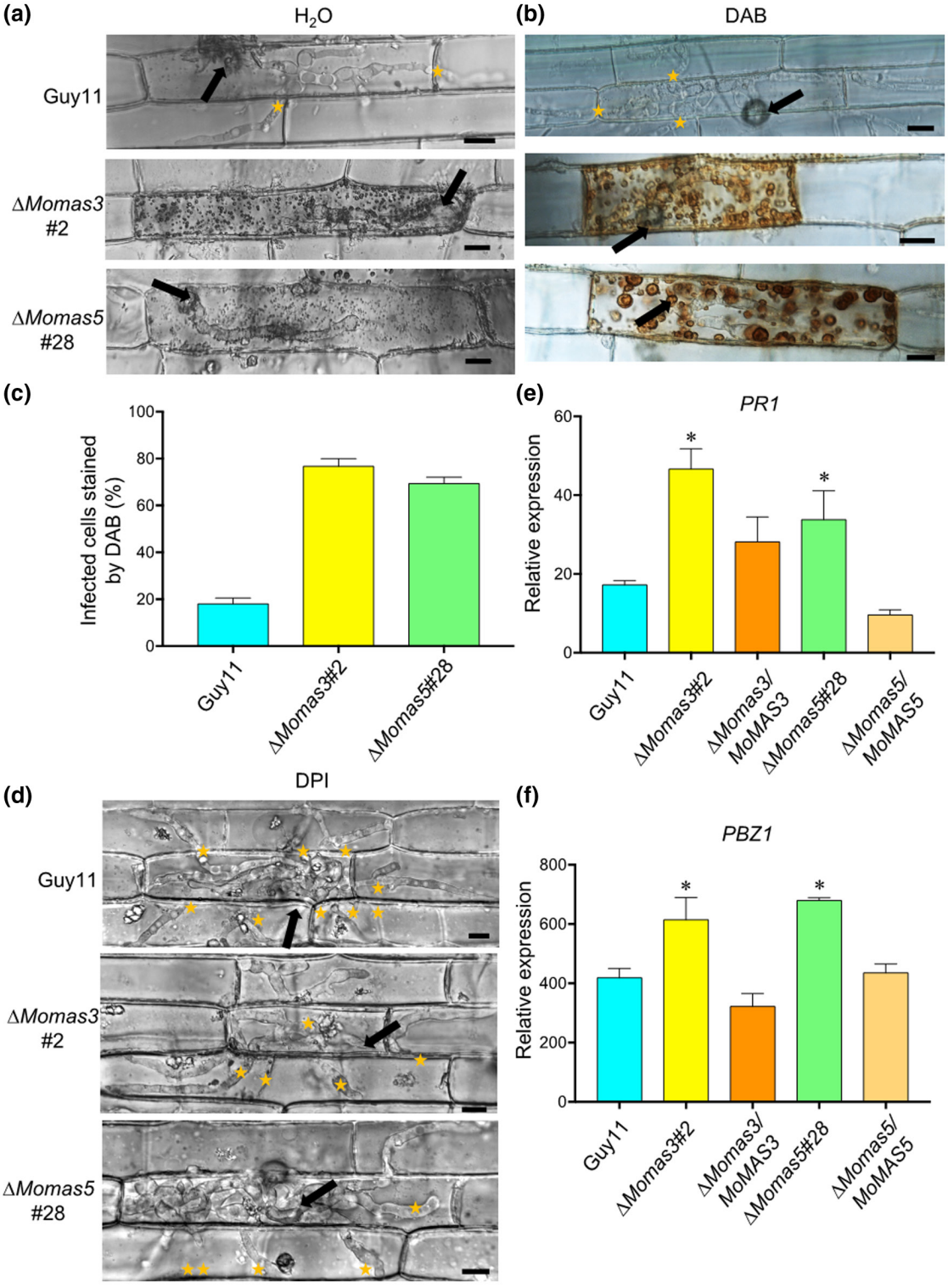

FIGURE 8 MoMas3 and MoMas5 are involved in suppressing the plant immune response. (a) Restriction of invasive hyphae and black compounds in rice cells infected with Δ*Momas3*#2 and Δ*Momas5*#28 mutant was observed at 40 h postinoculation (hpi). (b) Rice leaf sheaths infected with *Magnaporthe oryzae* wild-type Guy11, Δ*Momas3*#2, and Δ*Momas5*#28 mutant stained with 1 mg/ml 3,3′-diaminobenzidine (DAB). (c) Percentage of infected rice cells stained by DAB in *M. oryzae* wild-type Guy11, Δ*Momas3*#2, and Δ*Momas5*#28 strains. (d) A conidial suspension of the indicated strains treated with 0.4 μM diphenyleneiodonium (DPI) was injected into rice leaf sheaths and the results were observed at 42 hpi. Black arrows indicate appressoria. Yellow stars represent invasive hyphae invading neighbouring cells. Bar = 10 μm. (e, f) The transcription level of *PR1* and *PBZ1* in rice leaf sheaths infected with the indicated strains measured by reverse transcription-quantitative PCR. RNA samples were collected from rice leaf sheaths inoculated with wild-type Guy11, Δ*Momas3*#2, Δ*Momas5*#28 mutant, and complementation strains at 36 hpi. Error bars represent standard deviations and asterisks indicate significant differences ($p < 0.05$) based on Student's *t* test

Thus, the suppression of plant-derived ROS accumulation by DPI rescued the invasive hyphae biotrophic growth defect of Δ*Momas3* and Δ*Momas5* mutants.

We further examined the expression levels of pathogenesis-related rice genes *PBZ1* and *PR1* at 36 hpi in detached rice leaf sheaths. *PBZ1* and *PR1* expression are markers of the jasmonic acid pathway and the salicylic acid pathway, respectively (Campbell & Ronald, 2005; Dong et al., 2015; Hong et al., 2019). RT-qPCR results showed that the transcript levels of *PBZ1* and *PR1* were higher in leaf sheaths infected with the Δ*Momas3* and Δ*Momas5* mutants than in those infected with the WT and complementation strains (Figure 8e,f). In summary, we suggest that the Δ*Momas3* and Δ*Momas5* mutants were defective in suppressing ROS accumulation in rice cells and induced stronger plant defences against fungal colonization.

3 | DISCUSSION

Gas1 and Gas2, which are named as MAS proteins, function as virulence factors and were first reported in 2002. Gas1 and Gas2 are highly expressed in the appressorium formation stage and are required for penetration and full virulence of *M. oryzae* (Xue et al., 2002). In the present study, we found that six orthologous genes encode the MoMas protein family in *M. oryzae*; they all contain an N-terminal signal peptide, are rich in Ala and Gly residues, and share a conserved domain of unknown function (DUF) (Figures S1 and S2). Phylogenetic analysis showed that with homologs of *MAS* genes from other fungi, *MoMAS1*, *MoMAS2*, and *MoMAS3* are closest to *MoMAS4*, *MoMAS5*, and *MoMAS6*, respectively. Although Gas1 and Gas2 were identified, the roles of the other four MoMas proteins were unclear.

To better understand the function of the four MoMas proteins, we first knocked out all target genes and found that *MoMAS3*, *MoMAS4*, *MoMAS5*, and *MoMas6* were not necessary for fungal mycelial growth, conidiation, spore germination, and appressorium formation. However, *MoMAS3* and *MoMAS5* single deletion mutants showed reduced pathogenicity (Figure 1), whereas *MoMAS4* and *MoMAS6* deletion mutants showed similar pathogenicity (Figure S5) to the WT strain by spray inoculation and leaf sheath experiments. A previous study showed that the deletion of *MoMAS3* (MGG_00703) in the *M. oryzae* WT strain Ina72 does not affect virulence in the susceptible rice cultivar Shin No. 2 (Saitoh et al., 2012). However, infected leaves were not shown and statistical analysis of lesion counts was not performed in that study. Here, we knocked out *MoMAS3* in the *M. oryzae* WT strain Guy11 and the pathogenicity experiment was performed in the susceptible rice cultivar CO-39 with more than three biological repeats, with 20 infected leaves used for the statistical analysis to confirm the reduction of virulence in Δ*Momas3* mutants. Our results were also similar to those observed for Δ*Mogas1* and Δ*Mogas2* mutants. Thus, loss of *MoMAS3* results in reduced virulence (Xue et al., 2002). We concluded that *MoMAS3* and *MoMAS5* are required for full virulence of *M. oryzae*. Surprisingly, the Δ*Momas3*/Δ*Momas5* double mutants had a phenotype similar to that of the Δ*Momas3* and Δ*Momas5* single mutants (Figure S6). Similarly, a previous study demonstrated that there was no additional effect observed in Δ*Mogas1*/Δ*Mogas2* double mutants compared to the single deletion of Δ*Mogas1* and Δ*Mogas2* mutants (Xue et al., 2002).

Interestingly, MoMas3 and MoMas5 have different subcellular localization patterns, although they both localized to appressoria during the appressorium formation stage. The MoMas3-GFP fusion protein localized to the septum and cytoplasm in the conidial stage, while MoMas5-GFP had no signal in the conidia (Figures 4, 5 and S7). During the biotrophic infection stage, MoMas3-GFP completely outlined the invasive hyphae, suggesting it might be an apoplastic effector (Khang et al., 2010; Mosquera et al., 2009). Previous studies have reported that BFA can be used to inhibit the secretion of apoplastic effectors (Giraldo et al., 2013). After a leaf sheath infected by the MoMas3-GFP strain was treated with 10 μg/ml BFA for 3 h, the green signals remained inside the invasive hyphae instead of outlining the invasive hyphae (Figure 6); thus, we reasoned that MoMas3 is an apoplastic effector. However, MoMas5 was constitutively expressed in appressoria and weak signals were observed in the penetration peg at the early infection stage, but no signal was observed in invasive hyphae or inside plant cells. Based on these results, we suggest that MoMas5 functions as a virulence factor, similar to Gas1 and Gas2 (Xue et al., 2002).

How might MoMas3 and MoMas5 suppress plant defences? To determine the underlying mechanism of the deletion of *MoMAS3* and *MoMAS5* reducing pathogenicity, the leaf sheath assay was performed in Δ*Momas3*, Δ*Momas5*, and Guy11 strains. Our data showed that the invasive hyphae of the mutant strains were restricted to the first infected cell at 36 hpi. DAB staining indicated that ROS accumulated in rice cells infected with Δ*Momas3* and Δ*Momas5* mutants; inhibition of the ROS accumulation by DPI restored the expansion of invasive hyphae. The *PR* gene expression level in inoculated rice leaf sheaths revealed that the disruption of *MoMAS3* and *MoMAS5* induced plant immunity against infection (Figure 8). These results are consistent with the function of Gas1 and Gas2 homologs, EWCAs, in powdery mildew fungi, where the DUF domain contains a Gly 110 residue that interacts with chitin molecules (Martínez-Cruz et al., 2021). EWCAs have been identified as chitin active proteins that are involved in suppressing plant immunity by breaking down chitin oligomers to avoid recognition by PRRs. RNAi silencing of *PEC* genes resulted in restriction of invasive hyphae, ROS accumulation, and callose deposition in plant tissue (Martínez-Cruz et al., 2021). Pathogens produce and secrete diverse effectors to manipulate plant immunity for facilitating colonization (Oliveira-Garcia & Valent, 2015). The chitinase MoChi1 is an apoplastic effector and has been reported to be critical for full virulence and involved in suppressing the plant immune response. MoChi1 interacts with and competes with *OsMBL1* for chitin binding and suppresses the chitin-induced ROS burst in rice cells (Han et al., 2019). The chitinase MoChia1 is required for the growth, virulence, and development of *M. oryzae*, and also

functions as a PAMP to induce callose deposition in rice cell walls. MoChia1 suppresses the chitin-triggered ROS in rice, whereas OsTPR1 abolishes this suppression via interacting with MoChia1 to interfere with the binding between MoChia1 and chitin (Yang et al., 2019). Based on these results, we speculate that MoMas3 and MoMas5 might act as chitinases, even though these two proteins have different subcellular localizations. MoMas3 perhaps functions in a similar way to the apoplastic effector MoChi1 in binding chitin and suppressing the chitin-induced ROS burst in the rice cell (Han et al., 2019). MoMas5 might also function as a chitin-binding protein, perhaps similar to MoAa91(Li et al., 2020a), and might be secreted via the unconventional secretion system into rice cells, presumably to bind chitin or its derivatives to suppress plant immunity. If so, MoMas3 and MoMas5 would suppress the triggering of PAMP immunity by preventing the detection of fungal chitin. However, further experiments are needed to determine how MoMas3 and MoMas5 are involved in chitinase activity to subvert plant immunity. In summary, our results suggest that *MoMAS3* and *MoMAS5* act as virulence factors that are required for full pathogenicity and are also involved in suppressing plant immunity.

4 | EXPERIMENTAL PROCEDURES

4.1 | Fungal strains and culture conditions

M. oryzae Guy11 is the WT strain that was used to generate all the mutants mentioned in this study. All *M. oryzae* strains were cultured on complete medium (CM; 6 g yeast extract, 3 g casamino acids, 3 g peptone, 10 g sucrose, solidified with 15 g agar in 1 L of distilled water) or oatmeal agar (OM; 30 g oatmeal and 15 g agar in 1 L distilled water) plates and incubated at 25°C with a 12/12-h dark/light cycle. Fungal mycelia were cultured in liquid CM at 26°C with shaking at 160 rpm and used to generate protoplasts or to extract RNA and genomic DNA. Preparation of protoplasts and the transformation method was described by Li et al. (2020b). All transformants were screened on TB3 medium (3 g yeast extract, 3 g casamino acids, 200 g sucrose, and 15 g agar in 1 L of distilled water) with 300 μg/ml hygromycin B or 650 μg/ml G418.

4.2 | Phylogenetic analysis of MoMas protein sequence and its homologs

M. oryzae MAS protein sequences were used for BLAST searches against the NCBI database (https://www.ncbi.nlm.nih.gov/) and the EnsemblFungi database (http://fungi.ensembl.org/index.html) to obtain all MAS protein sequences from different filamentous fungal species, including *C. graminicola*, *F. graminearum*, *N. crassa*, and *A. alternata*. The phylogenetic tree was constructed using the MEGA 7 program with 1000 bootstrap replicates and the neighbour-joining method.

4.3 | Deletion of *MoMAS* genes

The split-PCR strategy (Li et al., 2020b) for gene replacement was used to disrupt the *MoMAS* genes, as described below. First, we amplified approximately 1 kb upstream and downstream fragments of the *MoMAS* gene using primers 1F/2R and 3F/4R, respectively, and used primers HYG-F/HYG-R to amplify the hygromycin B phosphotransferase (*HPH*) sequences. Second, the amplicon was fused with *HPH* using double-joint PCR. The 2 kb upstream and 1.8 kb downstream fusion fragments were amplified with 1F/HYG-R1 and HYG-F1/4R primer sets. Finally, the fusion fragments were transformed into Guy11 protoplasts, and *MoMAS* was replaced by an *HPH* cassette by homologous recombination. The putative mutants were screened on TB3 agar with hygromycin B and then double-screened by PCR using OF/OR, UA/H853, and H4/DB.

4.4 | Vegetative growth and appressorium formation assay

For vegetative growth testing, 5-mm small blocks from all mutant strains and WT Guy11 were inoculated on fresh CM plates for 7 days at 25°C in the dark. Then, the diameter of each colony was measured using a Vernier caliper (Kwon et al., 2018). For the appressorium formation assay, mycelial plugs of all strains were cultured on OM plates for 10 days and incubated at 25°C in a 12/12-h dark/light cycle. Then, the spores were harvested by one-layer Miracloth filtration using distilled water to wash the spores. The concentration of conidial suspensions was adjusted to 5×10^4 spores/ml. Next, nine drops (20 μl) of conidial suspension were added to hydrophobic surface slides and incubated at 25°C in the dark for 24 h. Finally, the appressorium formation of each strain was analysed under a light microscope. All assays were repeated three times and every strain had three repetitions for each experiment.

4.5 | Complementation and EGFP construct preparation

All vectors were constructed using homologous recombination. For the complementation vector, named MoMas3-CFR, the entire *MoMAS3* genomic sequence, including its promoter region and terminator, was amplified from the Guy11 strain with Np-F/CR primers. For the enhanced green fluorescent protein (EGFP) construct, named MoMas3-GFP, the genomic sequence of *MoMAS3* containing its promoter and coding sequences (without stop codon) were cloned using the Np-F/GFP-R primer set. The ends of the PCR products contained 15–20 bases homologous to the pGTN vector. The purified PCR product was fused with linearized pGTN, which was digested with *Kpn*I and *Not*I (for complementation) or *Kpn*I and *Hin*dIII (EGFP construct) restriction enzymes. The reaction mixture was then transferred to *Escherichia coli* DH5α, screened for ampicillin resistance, and all colonies were checked using PCR and sequencing. A similar procedure was used to construct the MoMas5-CFR and MoMas5-GFP vectors.

4.6 | Infection assay

In the spray inoculation assays, spores were harvested from 10-day-old strains on an OM plate, and equal conidial suspensions (10^5 spores/ml in 0.1% Tween 20) were sprayed onto the surface of 3-week-old CO-39 rice seedlings (0.1% Tween 20 solution served as a control). The inoculated seedlings were incubated in a high-humidity chamber for 24 h at 25°C in the dark and were then placed in a 12/12 h light/dark photoperiod chamber at 25°C for 5–6 days. The disease lesions were visible on the surface of the leaves, which were cut and collected with scissors. The samples were photographed using a camera. Leaf samples were collected at 36 hpi to monitor the temporal expression of defence-related genes by RT-qPCR.

The leaf sheath inoculation assay was used to detect the subcellular localization and invasive hyphal growth. The protocol was described by Kankanala et al. (2007). Four-week-old CO-39 rice seedlings were used to prepare hollow leaf sheaths, which were injected with equal concentrations of conidial suspensions (5×10^4 conidia/ml in 0.1% Tween 20). The inoculated leaf sheaths were placed in a sealed box with several layers of wet paper to keep them moist and incubated at 25°C in the dark. At the indicated time points after inoculation, the insides of leaf sheaths exposed to fungal conidia were excised for observation under the microscope.

4.7 | DAB staining

DAB (Sigma-Aldrich) staining was performed as described by Fernandez et al. (2014) and Li et al. (2020c). Briefly, samples from infected leaf sheaths at 36 hpi were sliced and soaked in 1 mg/ml DAB solution, then placed in the dark at room temperature for 8 h. After incubation, the samples were washed with ethanol:acetic acid solution (94:4 vol/vol) for 2 h and finally observed under a light microscope.

4.8 | DPI treatment

For the DPI (Toronto Research Chemicals) treatment assay, we first prepared a 10 mM DPI stock and then diluted it to 0.4 μM in a 0.2% gelatin solution. Spores were harvested and suspended in 0.4 μM DPI gelatin solution. Next, the conidial suspension was injected into the leaf sheath. Samples were placed in an incubator at 25°C in the dark for 42 h. After treatment, the samples were sectioned and examined under a light microscope.

4.9 | RT-PCR, RT-qPCR, and gene expression analysis

For RT-PCR, RNA was reverse transcribed into first-strand cDNA using a reverse transcription kit (Vazyme). All gene primers sets are listed in Table S2. RT-qPCR was performed using an Applied Biosystems 7500 real-time PCR system. The relative quantification of the transcriptional levels of all *MoMAS* genes was normalized to that of *actin* (MGG_03982). The expression levels of *PR1* and *PBZ1* were normalized to rice *actin* (LOC_Os10g36650).

4.10 | Microscopic observations

All microscopic observations (with or without fluorescence) were conducted using an Eclipse NI-E upright microscope (Nikon). For the detection of green fluorescence, EGFP was excited at a wavelength of 488 nm and detected at 505–550 nm.

ACKNOWLEDGEMENTS

This work was financially supported by grants from the Pests and Diseases Green Prevention and Control Major Special Project (110202101045 [LS-05]) and the Agricultural Science and Technology Innovation Program (ASTIP). Z.G. was supported by funding from the China Scholarship Council (file no. 201903250119).

DATA AVAILABILITY STATEMENT

The data that support the finding of this study are available from the corresponding author upon reasonable request.

ORCID

Wende Liu https://orcid.org/0000-0003-1506-9337

REFERENCES

Alvarez, M.E., Pennell, R.I., Meijer, P.J., Ishikawa, A., Dixon, R.A. & Lamb, C. (1998) Reactive oxygen intermediates mediate a systemic signal network in the establishment of plant immunity. *Cell*, 92, 773–784.

van den Burg, H.A., Harrison, S.J., Joosten, M.H., Vervoort, J. & de Wit, P.J. (2006) *Cladosporium fulvum* Avr4 protects fungal cell walls against hydrolysis by plant chitinases accumulating during infection. *Molecular Plant-Microbe Interactions*, 19, 1420–1430.

Campbell, M.A. & Ronald, P.C. (2005) Characterization of four rice mutants with alterations in the defence response pathway. *Molecular Plant Pathology*, 6, 11–21.

Chen, S., Songkumarn, P., Venu, R.C., Gowda, M., Bellizzi, M., Hu, J. et al. (2013) Identification and characterization of in planta-expressed secreted effector proteins from *Magnaporthe oryzae* that induce cell death in rice. *Molecular Plant-Microbe Interactions*, 26, 191–202.

Dong, Y., Li, Y., Zhao, M., Jing, M., Liu, X., Liu, M. et al. (2015) Global genome and transcriptome analyses of *Magnaporthe oryzae* epidemic isolate 98–06 uncover novel effectors and pathogenicity-related genes, revealing gene gain and lose dynamics in genome evolution. *PLoS Pathogens*, 11, e1004801.

Fernandez, J., Marroquin-Guzman, M., Nandakumar, R., Shijo, S., Cornwell, K.M., Li, G. et al. (2014) Plant defence suppression is mediated by a fungal sirtuin during rice infection by *Magnaporthe oryzae*. *Molecular Microbiology*, 94, 70–88.

Giraldo, M.C., Dagdas, Y.F., Gupta, Y.K., Mentlak, T.A., Yi, M., Martinez-Rocha, A.L. et al. (2013) Two distinct secretion systems facilitate tissue invasion by the rice blast fungus *Magnaporthe oryzae*. *Nature Communications*, 4, 1996.

Guo, M., Chen, Y., Du, Y., Dong, Y., Guo, W., Zhai, S. et al. (2019) The bZIP transcription factor *MoAP1* mediates the oxidative stress

response and is critical for pathogenicity of the rice blast fungus *Magnaporthe oryzae*. *PLoS Pathogens*, 7, e1001302.

Han, Y., Song, L., Peng, C., Liu, X., Liu, L., Zhang, Y. et al. (2019) A *Magnaporthe* chitinase interacts with a rice Jacalin-related lectin to promote host colonization. *Plant Physiology*, 179, 1416–1430.

Heese, A., Hann, D.R., Gimenez-Ibanez, S., Jones, A.M.E., He, K., Li, J. et al. (2007) The receptor-like kinase *SERK3/BAK1* is a central regulator of innate immunity in plants. *Proceedings of the National Academy of Sciences of the United States of America*, 104, 12217–12222.

Hong, Y., Liu, Q., Cao, Y., Zhang, Y., Chen, D., Lou, X. et al. (2019) The *OsMPK15* negatively regulates *Magnaporthe oryza* and *Xoo* disease resistance via SA and JA signaling pathway in rice. *Frontiers in Plant Science*, 10, 752.

Islam, M.T., Croll, D., Gladieux, P., Soanes, D.M., Persoons, A., Bhattacharjee, P. et al. (2016) Emergence of wheat blast in Bangladesh was caused by a South American lineage of *Magnaporthe oryzae*. *BMC Biology*, 14, 84.

Jones, J.D. & Dangl, J.L. (2006) The plant immune system. *Nature*, 444, 323–329.

Kankanala, P., Czymmek, K. & Valent, B. (2007) Roles for rice membrane dynamics and plasmodesmata during biotrophic invasion by the blast fungus. *The Plant Cell*, 19, 706–724.

Khang, C.H., Berruyer, R., Giraldo, M.C., Kankanala, P., Park, S.Y., Czymmek, K. et al. (2010) Translocation of *Magnaporthe oryzae* effectors into rice cells and their subsequent cell-to-cell movement. *The Plant Cell*, 22, 1388–1403.

Kwon, S., Lee, J., Jeon, J., Kim, S., Park, S.Y., Jeon, J. et al. (2018) Role of the histone acetyltransferase Rtt109 in development and pathogenicity of the rice blast fungus. *Molecular Plant-Microbe Interactions*, 31, 1200–1210.

Lamb, C. & Dixon, R.A. (1997) The oxidative burst in plant disease resistance. *Annual Review of Plant Physiology and Plant Molecular Biology*, 48, 251–275.

Li, G., Qi, X., Sun, G., Rocha, R.O., Segal, L.M., Downey, K.S. et al. (2020c) Terminating rice innate immunity induction requires a network of antagonistic and redox-responsive E3 ubiquitin ligases targeting a fungal sirtuin. *New Phytologist*, 226, 523–540.

Li, Y., Liu, X., Liu, M., Wang, Y., Zou, Y., You, Y., et al. (2020a). *Magnaporthe oryzae* auxiliary activity protein MoAa91 functions as chitin-binding protein to induce appressorium formation on artificial inductive surfaces and suppress plant immunity. *mBio*, 11, e03304–19.

Li, Z., Wu, L., Wu, H., Zhang, X., Mei, J., Zhou, X. et al. (2020b) Arginine methylation is required for remodelling pre-mRNA splicing and induction of autophagy in rice blast fungus. *New Phytologist*, 225, 413–429.

Marroquin-Guzman, M., Hartline, D., Wright, J.D., Elowsky, C., Bourret, T.J. & Wilson, R.A. (2017) The *Magnaporthe oryzae* nitrooxidative stress response suppresses rice innate immunity during blast disease. *Nature Microbiology*, 2, 17054.

Martínez-Cruz, J.S., Romero, D., Hierrezuelo, J.S., Thon, M., de Vicente, A., Pérez-García, P. et al. (2021) Effectors with chitinase activity (EWCAs), a family of conserved, secreted fungal chitinases that suppress chitin-triggered immunity. *The Plant Cell*, 33, 1319–1340.

Mentlak, T.A., Kombrink, A., Shinya, T., Ryder, L.S., Otomo, I., Saitoh, H. et al. (2012) Effector-mediated suppression of chitin-triggered immunity by *Magnaporthe oryzae* is necessary for rice blast disease. *The Plant Cell*, 24, 322–335.

Mosquera, G., Giraldo, M.C., Khang, C.H., Coughlan, S. & Valent, B. (2009) Interaction transcriptome analysis identifies *Magnaporthe oryzae* BAS1-4 as Biotrophy-associated secreted proteins in rice blast disease. *The Plant Cell*, 21, 1273–1290.

Orbach, M.J., Farrall, L., Sweigard, J.A., Chumley, F.G. & Valent, B. (2000) A telomeric avirulence gene determines efficacy for the rice blast resistance gene *Pi-ta*. *The Plant Cell*, 12, 2019–2032.

Oliveira-Garcia, E. & Valent, B. (2015) How eukaryotic filamentous pathogens evade plant recognition. *Current Opinion in Microbiology*, 26, 92–101.

Ou, S.H. (1985) *Rice diseases*. Wallingford, United Kingdom: CABI.

Rocha, R.O. & Wilson, R.A. (2020) *Magnaporthe oryzae* nucleoside diphosphate kinase is required for metabolic homeostasis and redox-mediated host innate immunity suppression. *Molecular Microbiology*, 114, 789–807.

Saitoh, H., Fujisawa, S., Mitsuoka, C., Ito, A., Hirabuchi, A., Ikeda, K. et al. (2012) Large-scale gene disruption in *Magnaporthe oryzae* identifies MC69, a secreted protein required for infection by monocot and dicot fungal pathogens. *PLoS Pathogens*, 8, e1002711.

Wang, J., Du, Y., Zhang, H., Zhou, C., Qi, Z., Zheng, X. et al. (2013) The actin-regulating kinase homologue MoArk1 plays a pleiotropic function in *Magnaporthe oryzae*. *Molecular Plant Pathology*, 14, 470–482.

Wang, J., Yin, Z., Tang, W., Cai, X., Gao, C., Zhang, H. et al. (2017) The thioredoxin MoTrx2 protein mediates reactive oxygen species (ROS) balance and controls pathogenicity as a target of the transcription factor MoAP1 in *Magnaporthe oryzae*. *Molecular Plant Pathology*, 18, 1199–1209.

Wilson, R.A. (2021) *Magnaporthe oryzae*. *Trends in Microbiology*, 29, 663–664.

Wilson, R.A. & Talbot, N.J. (2009) Under pressure: investigating the biology of plant infection by *Magnaporthe oryzae*. *Nature Reviews Microbiology*, 7, 185–195.

Xue, C., Park, G., Choi, W., Zheng, L., Dean, R.A. & Xu, J.R. (2002) Two novel fungal virulence genes specifically expressed in appressoria of the rice blast fungus. *The Plant Cell*, 14, 2107–2119.

Yang, C., Yu, Y., Huang, J., Meng, F., Pang, J., Zhao, Q. et al. (2019) Binding of the *Magnaporthe oryzae* chitinase MoChia1 by a rice tetratricopeptide repeat protein allows free chitin to trigger immune responses. *The Plant Cell*, 31, 172–188.

Zhang, H., Fang, Q., Zhang, Z., Wang, Y. & Zheng, X. (2009) The role of respiratory burst oxidase homologues in elicitor-induced stomatal closure and hypersensitive response in *Nicotiana benthamiana*. *Journal of Experimental Botany*, 60, 3109–3122.

SUPPORTING INFORMATION

Additional supporting information may be found in the online version of the article at the publisher's website.

How to cite this article: Gong, Z., Ning, N., Li, Z., Xie, X., Wilson, R.A. & Liu, W. (2022) Two *Magnaporthe* appressoria-specific (MAS) proteins, MoMas3 and MoMas5, are required for suppressing host innate immunity and promoting biotrophic growth in rice cells. *Molecular Plant Pathology*, 23, 1290–1302. https://doi.org/10.1111/mpp.13226